2.4 *Linac*

P.N. Ostroumov, Physics Division, ANL
November 8, 2004

Accelerating cavities

Experiments with IH resonator at CERN show the possibility of obtaining high electric fields in IH resonators [1]. At 200 MHz operating frequency the maximum effective accelerating gradient was 10.7 MV/m. This corresponds to a local field maximum of 75 MV/m, and to fields in excess of 50 MV/m (3.5 times the Kilpatrick limit) on large portions of the drift tube surfaces. The average field in the accelerating gap was 30 MV/m. The pulse length in this experiments was in the range from 100 μs to 1 ms.

For the HEDP driver application a 50 MHz 3-gap IH-resonators can be effectively applied. The accelerating gap length depends on the beam velocity and will be in the range of ~2-5 cm. At low frequency the Kilpatrick limit only slightly depends upon the gap length and it is 9.5 MV/m for 50 MHz and gap length ~2 cm. The CERN IH resonator has small diameter drift tubes therefore the total surface area under high electric field is small. In the HEDP driver resonator the surface area is much larger due to the multi-channel feature. From other side, the pulse length can be very short and close to the resonator filling time which is ~20 μs for Q_0 =3000. We assume peak surface field in the HEDP resonators less than ~3.2 Kilpatrick limit which is slightly lower than in the CERN IH resonator. This assumption results in a peak surface field 30 MV/m and average field in the gap ~18 MV/m. However, there is no need to operate all resonators at the highest possible fields because the field level can be limited by beam loading.

A more reasonable scenario is to operate all resonators to provide equal voltage gain ~ 1MV. In this case the energy transferred to the beam is less than10% of the stored energy as is seen form Table 1. The electrodynamics calculations of the resonators have been performed by the CST MWS code. Figure 1 and 2 show some views of the IH resonator designed for 100 keV/u and 1 MeV/u ion beam. Large-surface drift tubes are suitable to locate 16 beam apertures in two rows (only one aperture hole at the center of the cavity is shown in Fig. 1). For simplicity of the design and simulations a rectangular cross-section has been assumed. The surface area of the drift tube is 90x18 cm^2 which is sufficient to locate 2 rows of aperture holes, 8 holes in each row. Figure 2 shows the intensity of the electric field in the accelerating gaps of the resonator at the high-energy end of the linac. The distribution of the E_z field in the first resonator is shown in Fig. 3.

Table 1

Input energy	0.1 MeV/u	0.95 MeV/u
Q (copper)	3588	6950
Stored energy	16 J	~16 J
Power to achieve total voltage gain 1 MV	160 kW	80 kW
Energy transferred to beam with the pulse length 200 nsec and current 5 A	1.0 J	1.0 J

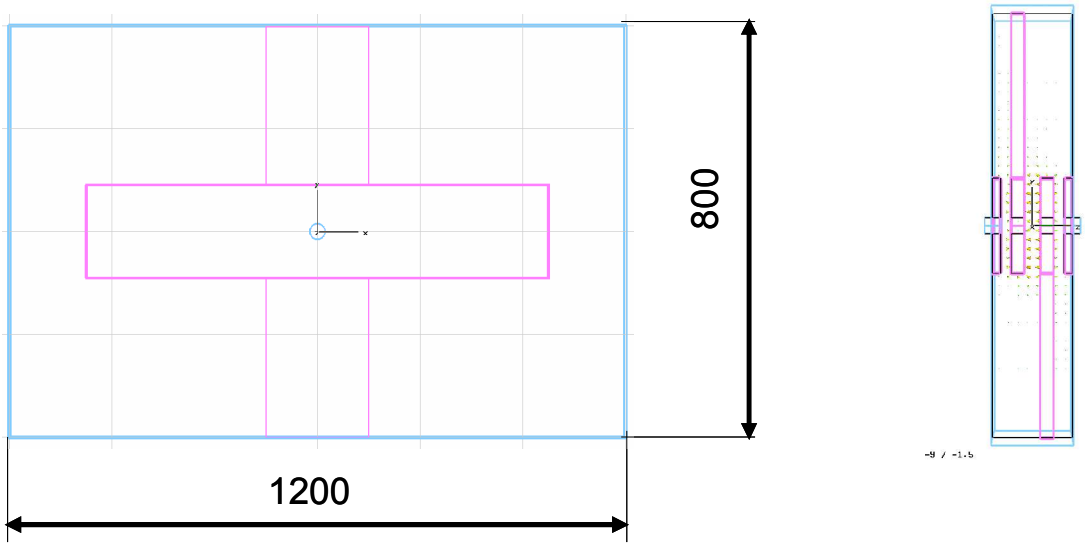

Figure 1. Plane and side views of the 3-gap IH resonator. The dimensions are in mm.

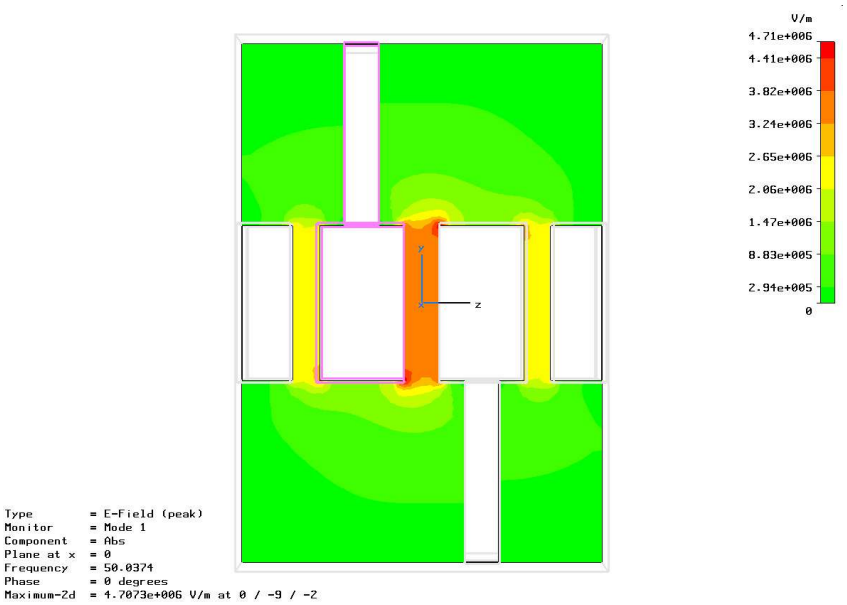

Figure 2. Side view of the 3-gap IH resonator designed for beta=0.01465.

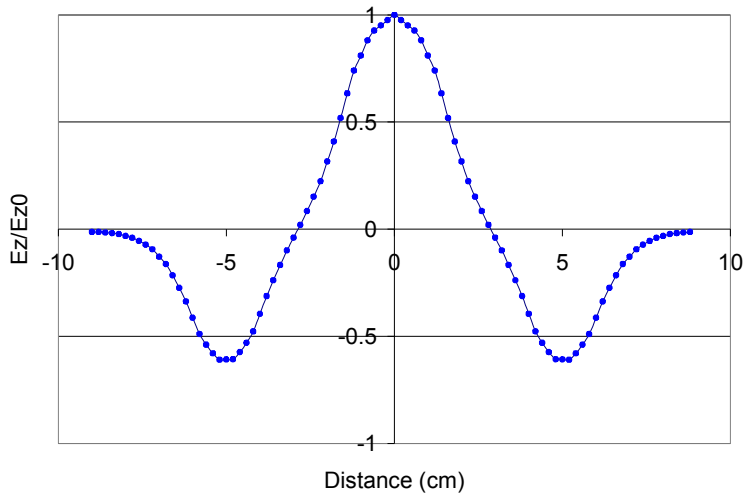

Figure 3. E_z along the resonator #1.

Design of the linac

The linac has been designed using TRACE-3D [2]. The main assumptions are:

1) Focusing by ~15 Tesla solenoids following each resonator;
2) Total voltage gain in each resonator is 1.2 MV. The voltage is limited by the peak surface field in the first resonator and beam loading in all other resonators;
3) Synchronous phase is φ_S=-30° except in the first two resonators where φ_S =-40°.
4) For each of 16 beamlet the normalized transverse emittance (5σ) is 5 π mm·mrad. Longitudinal emittance (5σ) is 5000 keV·deg.

Main parameters of the linac are given in Table 2

Table 2. Main parameters of the linac.

Beam	$^{20}Ne^{1+}$
Input energy	2 MeV, 0.1 MeV/u
Output energy	20 MeV, 1 MeV/u
Current	300 mA
Frequency	50 MHz
Length	8.6 m
Number of resonators	17
Voltage per gap	400-500 kV
Type of resonator	3-gap IH
Field in the solenoids	15 Tesla
Effective length of the solenoids	15 cm

Figure 4 shows TRACE-3D screen of the $^{20}Ne^{1+}$ beam simulation in the linac. Beam current is 300 mA. The input file for TRACE-3D is attached. The solenoids provide strong focusing with small beam envelope modulation. Beam radius is less than 15 mm. According to the TRACE-3D calculations 600 mA neon beam can be accelerated in the linac with the same setting of solenoids.

To obtain smooth beam envelopes the initial Twiss parameters should be slightly changed with respect to 300 mA case as is seen from Fig. 5.

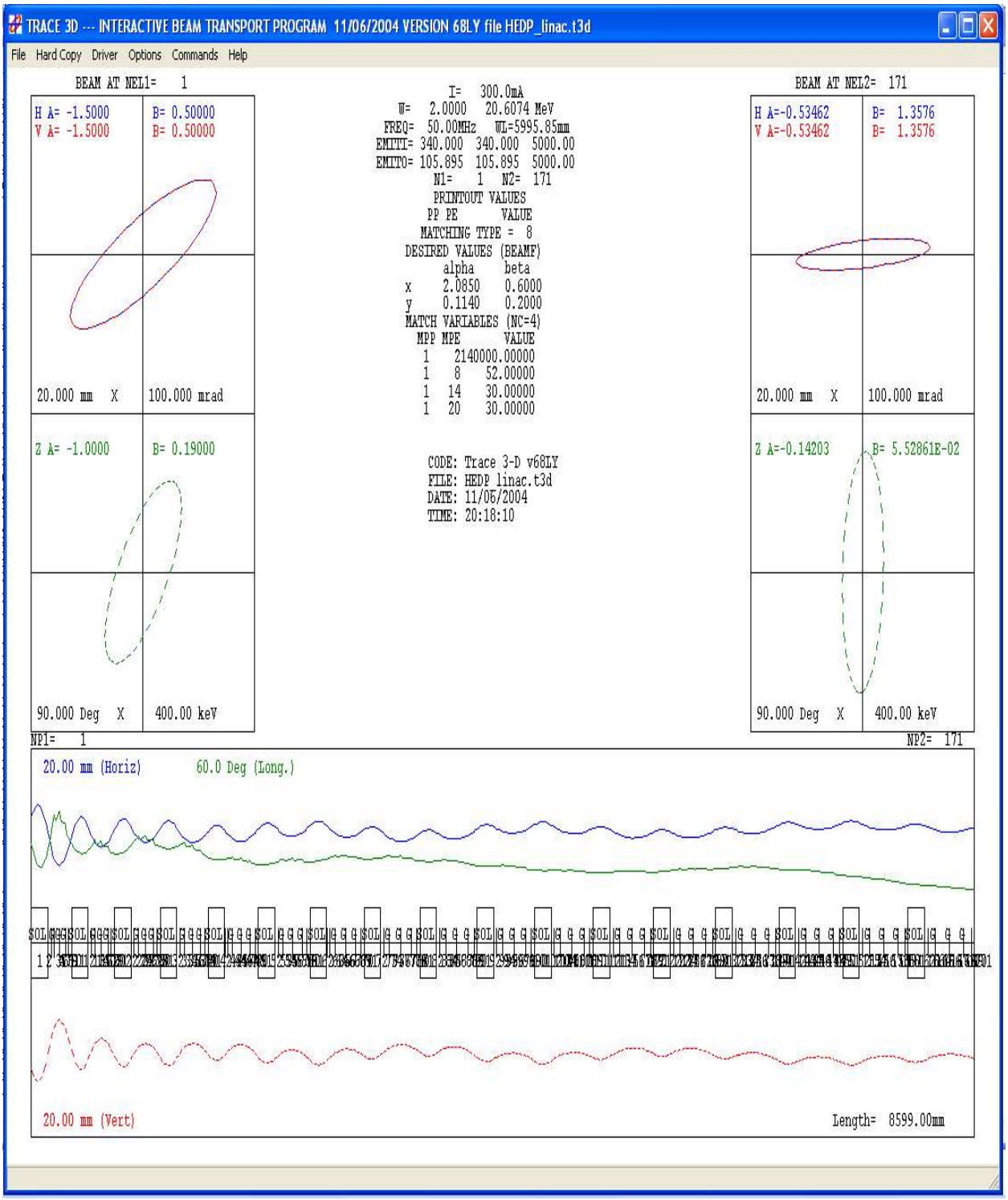

Figure 4. TRACE-3D screen of the linac lattice. Beam current is 300 mA. The blue curves show X-envelope, the red curves – Y-envelope and the green curves are the phase envelope.

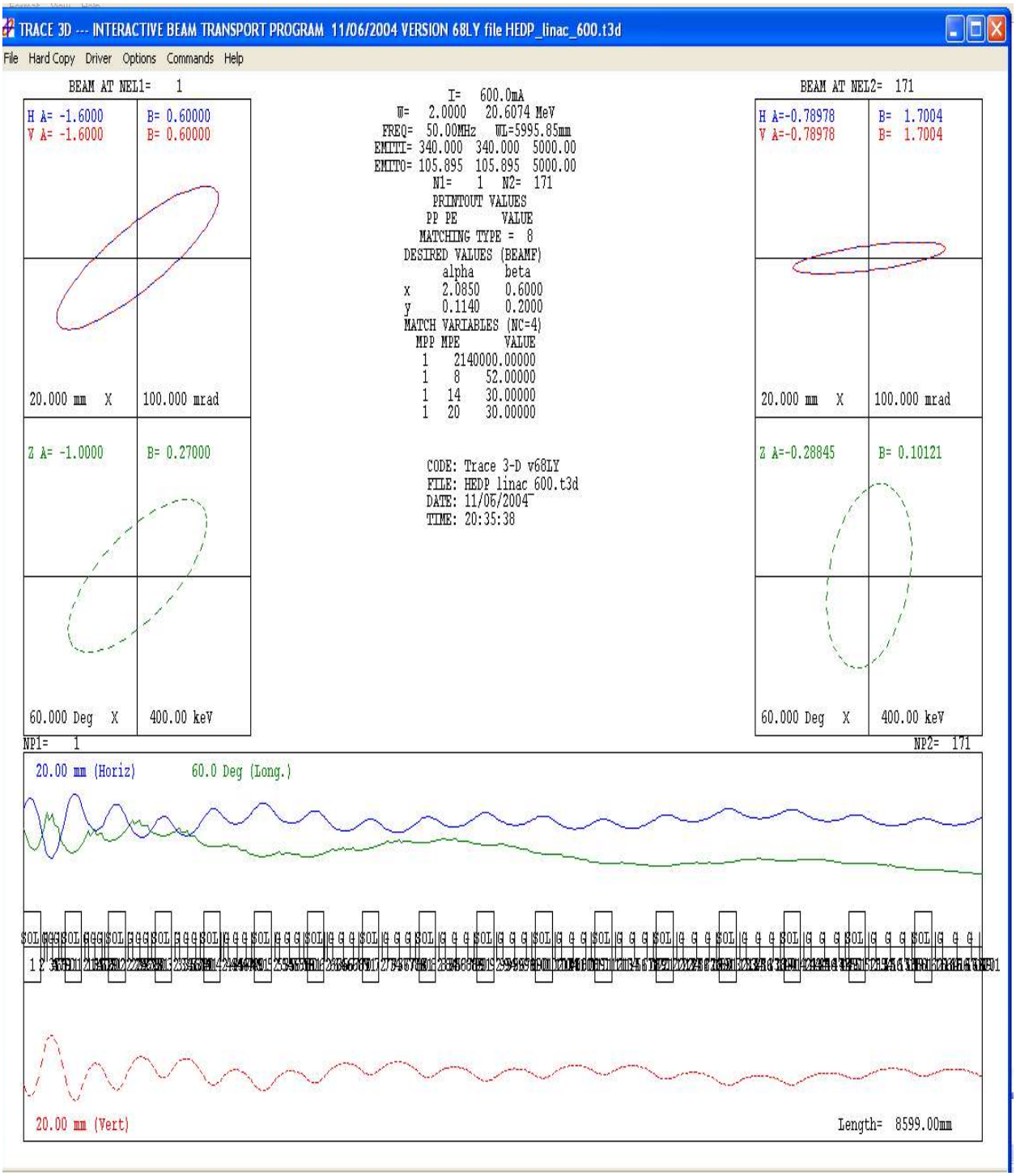

Figure 5. TRACE-3D screen of the linac lattice. Beam current is 600 mA.

Superconducting solenoids

High-field superconducting solenoids can be made with opposite directions of current flow as is shown in Fig. 6.

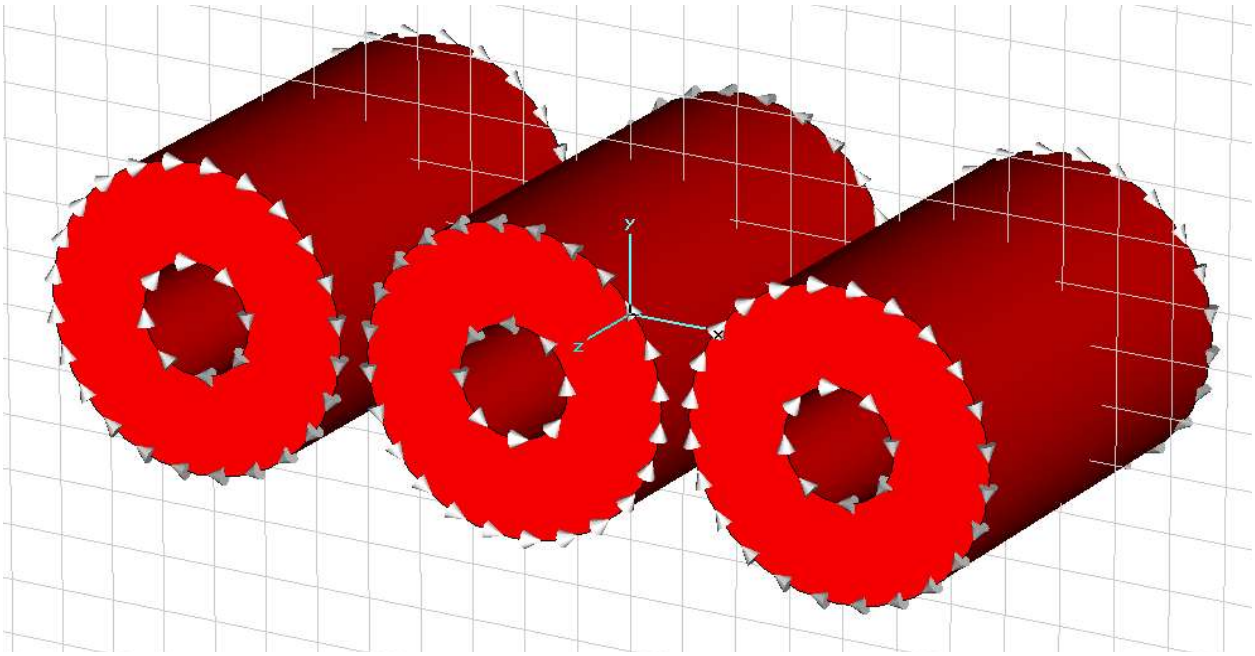

Figure 6. CST EM studio models of the solenoids.

Beam bunching

Bunching of high-current beam prior to injection into the linac can be performed using a standard "klystron" buncher technique. The buncher is a 3-gap IH resonator with total voltage 100 kV and located ~70 cm upstream of the first accelerating cavity. Beam dynamics simulations have been carried out for 100 keV/u 500 mA singly-charged neon beam. Fig. 7 shows evolution of the phase space plots along the buncher and drift space. Beam space charge prevents the effective bunching. However, 63% of a dc beam can be bunched into a phase width 100° as is shown in Fig. 8.

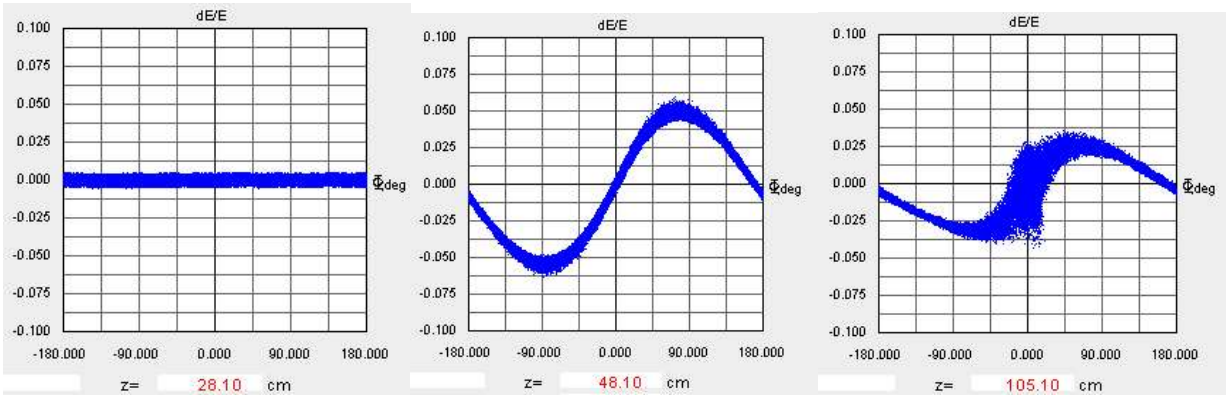

Figure 7. Longitudinal phase space plots of the beam during the bunching.

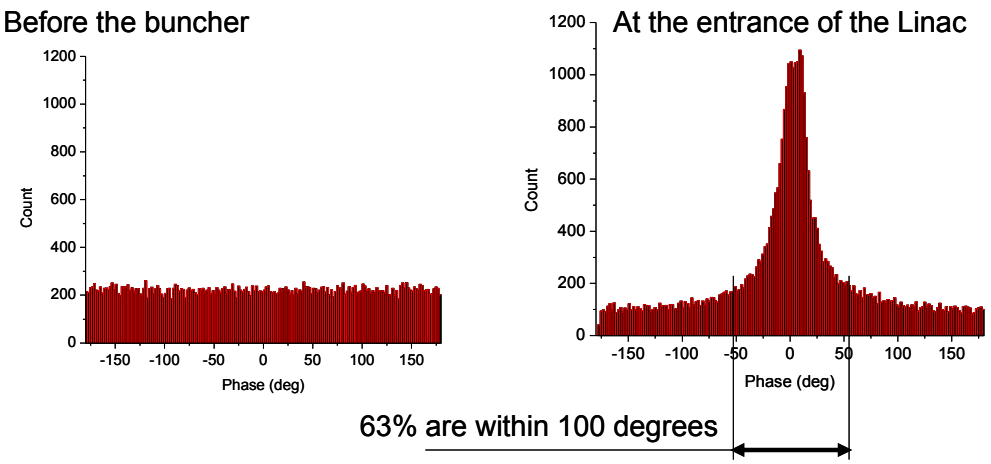

Figure 8. Bunch phase spectrum before the buncher and at the entrance of the linac.

Beam debunching

At the exit of the linac the beam pulse length is 200 nsec and consists of 10 short bunches. The time width of each bunch is ~ 2.2 nsec. The dynamics of the neon beam debunching in the drift space downstream of the linac has been simulated by the TRACK code [3]. The simulation has been performed using full 3D external and space charge fields. The solenoids were represented by 3D fields obtained from CST EM-Studio code. Figure 9 shows the phase space plots of the beam exiting the linac and post-linac 4.46 m transport system containing solenoids and debuncher. The energy spread of the beam is ±1%. Due to strong space charge forces the beam energy spread increases in the drift space upstream of the debuncher. The debuncher is a 3-gap IH resonator with the voltage 0.7 MV. In this simulation the debuncher is a single-harmonic resonator operating at 50 MHz. Therefore the beam phase space plots show strong nonlinear shape of the beam longitudinal phase space plots as is seen from the bottom plots in Fig. 10. These non-linearity can be minimized using second and third harmonic debuncher resonators.

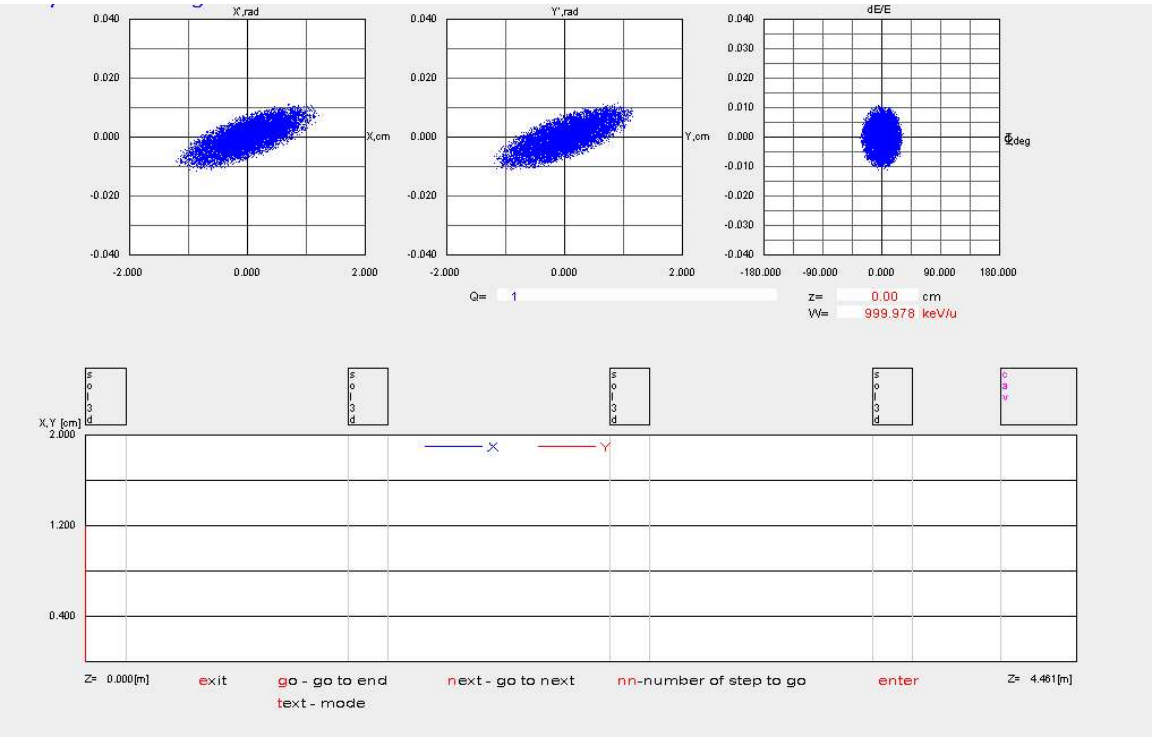

Figure 9. Beam phase space plots at the exit of the linac and transport line to the debuncher.

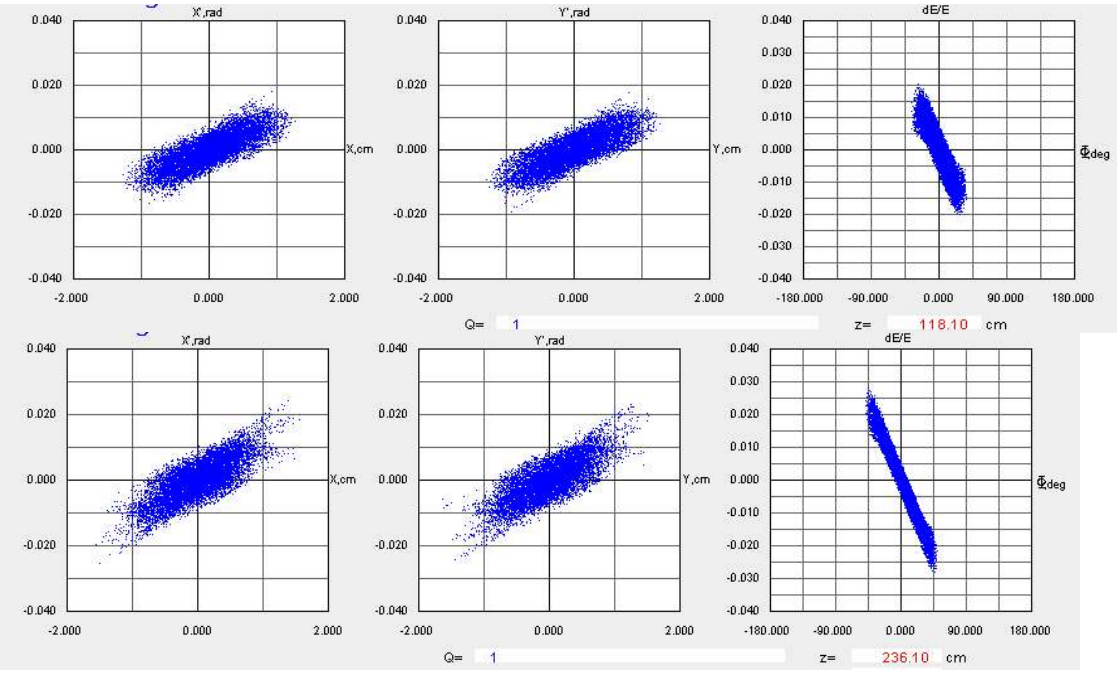

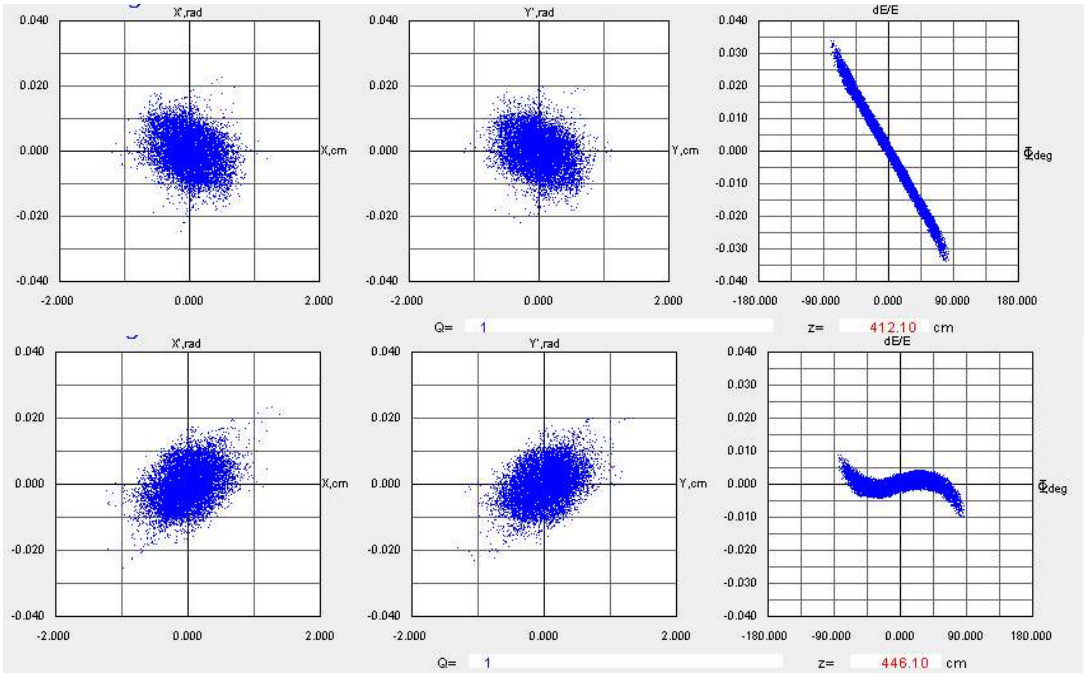

Figure 10. Evolution of bunched beam phase space plots in the drift space and effect of the debuncher.

Attachments

1. TRACE-3D input files for the linac (300 mA and 600 mA)
2. EXCEL file of the electric field distribution in the gap.

References

1. J.Broere et al. High Power Conditioning of the 202 MHz IH Tank 2 at the CERN Linac3. Proc. of the LINAC-98, p. 771.
2. K.R. Crandall, *TRACE 3-D Documentation,* Report LA-11054-MS, Los Alamos, 1987.
3. Ostroumov, P.N., Aseev, V. N., Mustapha, B., *Phys. Rev. ST. Accel. Beams,* Volume 7, 090101 (2004).